The square-triangle random-tiling model in the thermodynamic limit

1994 J. Phys. A: Math. Gen. 27 3599

(http://iopscience.iop.org/0305-4470/27/11/010)

J. Phys. A: Math. Gen. 27 (1994) 3599–3614. Printed in the UK

The square-triangle random-tiling model in the thermodynamic limit

P A Kalugin

Groupe de dynamique des phases condensées, Université Montpellier 2, place Eugene Bataillon, 34095 Montpellier, France
and
LD Landau Institute for Theoretical Physics, 117334, Kosygina St 2, Moscow, Russia

Received 15 December 1993

Abstract. The thermodynamic limit for the square-triangle random-tiling model is considered. The analytic solution of the Bethe-ansatz equations found recently by Widom is obtained. The *analytic* expression for entropy density as a function of the fraction of the plane occupied by triangles α_t is derived for the case $\alpha_t \geqslant \frac{1}{2}$, i.e. for the phason gradients having 6-fold symmetry, including 12-fold symmetric phase as the limiting case. The *exact* values for phason elastic constants are also found.

1. Introduction

The square-triangle random-tiling model belongs to the class of two-dimensional statistical mechanics problems, which deals with the coverings of the plane by rigid tiles. This class of models comprises, in particular, the dimer model [1] on a lattice and the hard-hexagon model [2]. The *exact solution* of them in the thermodynamic limit is usually taken to mean the analytic expression of the free energy as a function of a set of macroscopic parameters. Examples are the densities of the dimers of distinct orientations for the dimer model and the occupation factors of different sublattices for the hard-hexagon model. The correct choice of macroscopic parameters rests, however, as a matter of guesswork. As the square-triangle random tiling is commonly regarded as a model of the structure of the 12-fold symmetric quasicrystal (QC), it is reasonable to describe it by the macroscopic parameters borrowed from the theory of QC.

The model of the structure of quasicrystals based on the random tilings of the plane was originally suggested by Elser [3] as an alternative to the deterministic description of QC. The macroscopic parameter of order in the random-tiling QC models is called the phason field (see, e.g., [4]). In random-tilings the phason field is a fluctuating quantity, in contrast to the deterministic QC, where it is constant. By a widely believed hypothesis, these fluctuations on the large scale are described by the entropy-density quadratic in the phason gradient [5, 6]. One of the consequences of this hypothesis is that the *mean* entropy density is quadratic in the *mean* phason gradient, which is also called the *background phason strain* [4]. The results obtained below show, in particular, the validity of this conjecture for the square-triangle random-tiling model.

The space of background phason strains for the square-triangle tiling is three-dimensional, whereas the phason gradients of general tilings with 12-fold symmetry form a 4D space [7]. This peculiarity of the square-triangle tilings is due to a geometric constraint

0305-4470/94/113599+16$19.50

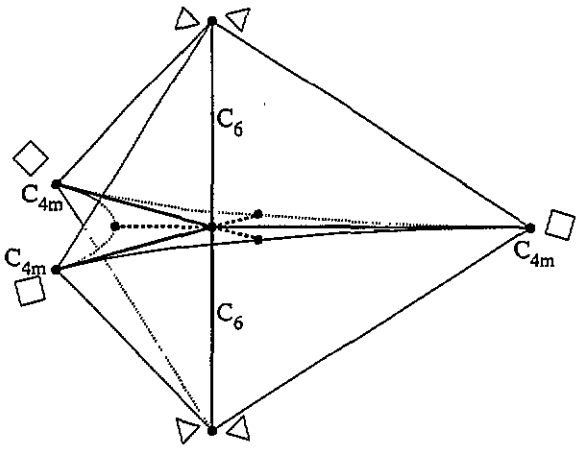

Figure 1. The region in the 3D space of phason gradients accessible to the square-triangle tilings. This region is bounded by curved surfaces; thin lines represent their edges. The vertices correspond to the ideal square and triangular lattices; the tiles constituent these lattices are shown nearby. Bold lines correspond to the phason gradients having 6-fold and 4-fold (with reflection) symmetries.

remarked in [4]. The phason strain of a tiling is bounded; roughly speaking it cannot exceed that of an individual tile. More precisely, phason gradients corresponding to tilings belong to the region of complex form shown on the figure 1. The 30 degree rotation in the plane of tiling acts on the space of phason strains by the rotation through 120 degrees and the reflection in the symmetry plane. Thus, this plane corresponds to the tilings with 4-fold symmetry. The additional requirement of the reflection symmetry is satisfied on three lines in this plane, whereas the 6-fold-symmetric tilings correspond to the line, perpendicular to it (see figure 1). Finally, the 12-fold symmetry demands the strain being equal to zero.

The thermodynamic parameters of random-tiling models of quasicrystals should not distinguish tiles of the same shape, but having different orientations. In the case of the square-triangle tiling the only independent parameter of this kind is the relative concentration of squares and triangles, or, say, the fraction of plane occupied by triangles α_t (see [8]). The parameter α_t depends on the phason strain. Zero gradient requires $\alpha_t = \frac{1}{2}$, and the maximum-entropy condition for $\alpha_t > \frac{1}{2}$ gives rise to tilings with 6-fold symmetry (at least for $\alpha_t - \frac{1}{2} \ll 1$, but the author supposes that this is true for all $\frac{1}{2} < \alpha_t < 1$).

2. Bethe-ansatz equations

As was shown in [4], the square-triangle random-tiling model allows the transfer-matrix description. However, the way the transfer matrix is introduced in [4] has the inconvenience that the squares of different orientations are transformed into figures of different areas. Thus, the area scaling factor depends not only on α_t. This means that the largest transfer-matrix eigenvalue does not correspond, in general, to the maximum of the entropy density for a given α_t. This difficulty can be eliminated by using another lattice representation of the model. The details of this representation are clear from an example of the transformed tiling shown in figure 2. The tiles are deformed in such a way that equilateral triangles are transformed into rectangular ones and $\pm 15°$ squares (see [8]) are transformed into parallelograms, while 45° squares rest unchanged. Because the vertices of the transformed

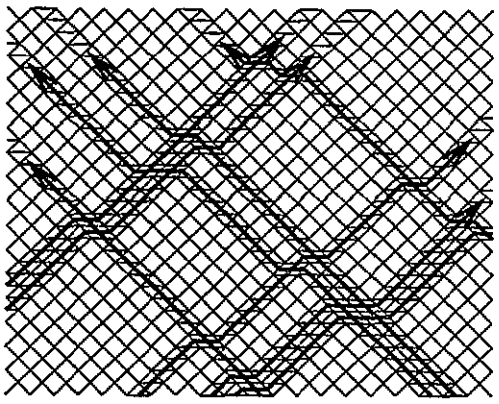

Figure 2. The lattice representation of the square-triangle tiling model. The world lines of right and left particles are shown by bold lines.

tiling form a square lattice rotated by 45°, it is possible to introduce the transfer matrix between the states on the neighbouring rows. This transfer matrix can be conveniently expressed in terms of left-moving and right-moving (henceforth *left* and *right*) particles, the world lines of which are shown in figure 2. Choose the unit of length in the 'space' and the unit of 'time' both equal to one-half diagonal of a square, the speed of free particles is thus equal to ± 1. All particles have at the same moment time coordinates of the same parity; the parity, however, changes from one row to another. The weights associated with freely moving particles are all equal to 1, but it is necessary to impose the weight factors equal to $\exp(\pm\phi)$ for two distinct ways of intersection of the world lines [4, 8]. This parameter is a thermodynamic conjugate to Δ, the average difference between the numbers of 'right' and 'left' intersections in a row [8].

It is worth mentioning here that we are dealing with the same particles as those introduced in [4, 8] and only their coordinates are transformed; more specifically, the coordinate of a particle is increased by the number of particles to the left of it. This fact permits using the same form of Bethe ansatz as that found in [8] for the eigenstates of the transfer matrix. Following [8], denote the amplitudes of plane waves by $A(\{k_i\})$, where $\{k_i\}$ stands for an ordered set of momenta of particles. These momenta are denoted by p_i and q_j for left and right particles, respectively. The sequence of p and q in $\{k_i\}$ matches the sequence of the particle species in the configurational space. From the preceding it may be seen that the eigenstates used here and those of [8] are described by the same set of momenta and differ only in the amplitudes $A(\{k_i\})$. The eigenvalues of the transfer matrix are thus the same:

$$\Lambda = \exp \mathrm{i}\left(\sum_i p_i - \sum_j q_j\right). \tag{1}$$

The equations for $A(\{k_i\})$ for the modified tiling follow from (3) and (4) of [8]:

$$\begin{aligned} A(\ldots, p_j, p_i, \ldots) &= -A(\ldots p_i, p_j, \ldots) \\ A(\ldots, p_i, q_k, \ldots) &= (\xi_i - \psi_j) A(\ldots, q_j, p_i, \ldots) \end{aligned} \tag{2}$$

where

$$\xi_i = \exp(2\mathrm{i}p_i + \phi) \qquad \psi_j = -\exp(-2\mathrm{i}q_j - \phi). \tag{3}$$

The equations (2) on the amplitudes $A(\{k_i\})$ define the eigenstates of the transfer matrix. The complete proof of this fact is presented in appendix A.

The periodic boundary conditions give rise to the following equations:

$$e^{-M\phi}\xi_i^M = (-1)^{n_+-1}\prod_j(\xi_i - \psi_j) \qquad e^{M\phi}\psi_j^M = (-1)^{M+n_--1}\prod_i(\xi_i - \psi_j) \tag{4}$$

where $2M$ is the length of a row, and n_- and n_+ are the numbers of right and left particles, respectively.

3. Exact solution in the thermodynamic limit

As the parity of M and $n_\pm$ is of no importance in the thermodynamic limit, one can drop the factors ± 1 in (4). If in the first of them ψ_j are considered as parameters, then $\{\xi_i\}$ are roots of the following equation in z:

$$e^{-M\phi}z^M = \prod_j(z - \psi_j)\,. \tag{5}$$

It is convenient to take a logarithm of (5):

$$M(-\phi + \log(z)) - \sum_j \log(z - \psi_j) = 0 \pmod{2\pi i}\,. \tag{6}$$

The real part of (6) determines a smooth closed curve in the plain of the variable z, which can consist of one or several components. In fact, at least while n_-/M is small enough, it consists of only one loop, and everywhere below only this case is considered. As an algebraic equation of the order M, equation (5) has M roots, hence the imaginary part of (6) gives M possible positions on this curve. Numerical calculations for small M show that Λ reaches its maximal value when ξ_i occupy n_+ successive positions without omission (see figure 3). The author supposes that this is true also in the thermodynamic limit, $M \to \infty, n_\pm/M \to$ constant. It is convenient to introduce the functions,

$$f_+(z) = 1/z - \lim_{M\to\infty} M^{-1}\sum_j \frac{1}{z - \psi_j} \qquad f_-(z) = 1/z - \lim_{M\to\infty} M^{-1}\sum_j \frac{1}{z - \xi_j}\,. \tag{7}$$

Differentiating (6) and taking into account the arrangement of ξ_i discussed above, we obtain

$$\lim_{M\to\infty} Mf_+(\xi_k)(\xi_{k+1} - \xi_k) = 2\pi i\,. \tag{8}$$

This expression and its analogue for $f_-(\psi_k)$ allow transforming the sum in (7) into an integral,

$$f_+(\zeta) = 1/\zeta + \frac{1}{2\pi i}\int_{b_+^*}^{b_+} \frac{f_-(z)dz}{z - \zeta} \qquad f_-(\zeta) = 1/\zeta - \frac{1}{2\pi i}\int_{b_-^*}^{b_-} \frac{f_+(z)dz}{z - \zeta} \tag{9}$$

where b_-, b_-^*, b_+ and b_+^* denote the thermodynamic limit for ξ_{n_+}, ξ_1, ψ_1 and ψ_{n_-} (the symmetry of $\{\xi_i\}$ and $\{\psi_j\}$ with respect to complex conjugation is required by the 'time'-reversal symmetry of the major eigenstate).

In the thermodynamic limit the points $\{\psi_j\}$ and $\{\xi_i\}$ approach the smooth curves Ψ and Ξ, which should be taken as the integration contours in (9). As the integration in (9) is analytic, the precise form of the contours is not important, while they get around the singularities of the integrands in the same way as Ψ and Ξ do. Generally, there are singularities at the points b_+, b_-, b_+^*, b_-^* and 0, but we should be careful, when Ψ and Ξ intersect each other. In this case the point of intersection, being singular for f_+ and f_-, 'pins' both contours. The numerical calculations, however, show no intersection of this sort for the case $b_+ = b_-$, which corresponds to the phases with $\alpha_t > \frac{1}{2}$, as shown below.

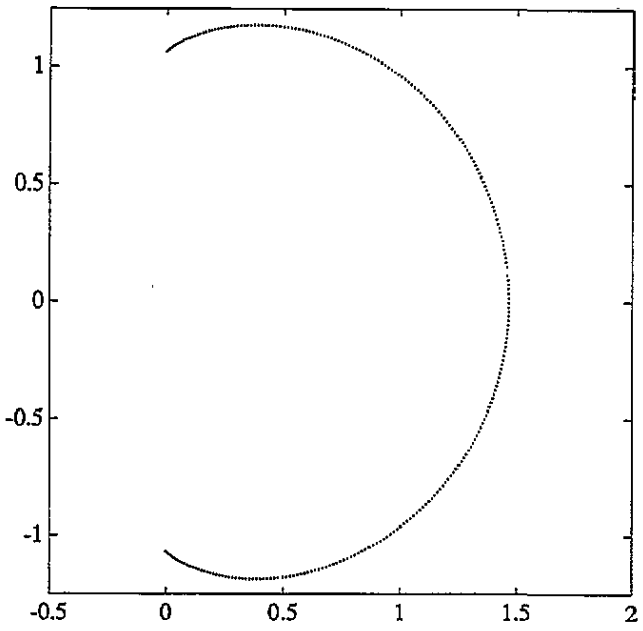

Figure 3. The distribution of $\{\xi_i\}$ for the largest eigenvalue of the transfer matrix. Numerical result for $M = 627$ and $n_\pm = 265$.

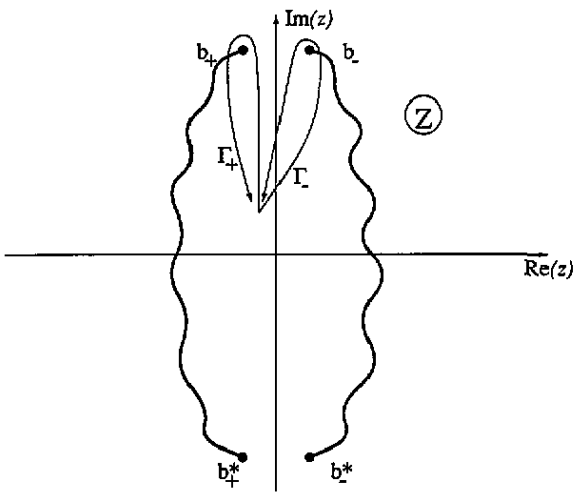

Figure 4. The monodromy group generators for the function $a_+ f_+(z) + a_- f_-(z)$.

Consider now the analytical properties of an arbitrary linear combination $a_+ f_+(z) + a_- f_-(z)$. Suppose, that the curves Ψ and Ξ do not intersect, and arrange two cuts in the plain of the variable z, having the same topology (see figure 4). Equations (9) give the monodromy transformation of this function with respect to the contours Γ_+ and Γ_-:

$$\Gamma_+ : \begin{pmatrix} a_+ \\ a_- \end{pmatrix} \to \begin{pmatrix} 1 & 0 \\ -1 & 1 \end{pmatrix} \begin{pmatrix} a_+ \\ a_- \end{pmatrix} \qquad \Gamma_- : \begin{pmatrix} a_+ \\ a_- \end{pmatrix} \to \begin{pmatrix} 1 & 1 \\ 0 & 1 \end{pmatrix} \begin{pmatrix} a_+ \\ a_- \end{pmatrix}. \quad (10)$$

These two matrices generate the whole group $SL(2, Z)$, which is thus the monodromy group of f_+ and f_-. The situation is significantly simplified if $b_+ = b_- = b$, when we deal with only one monodromy generator $\Gamma_+\Gamma_-$. Fortunately, as shown below, this case corresponds to tilings having 6-fold symmetry, and, particularly, to the 12-fold-symmetric tiling. Everywhere below we consider only this case. Because $(\Gamma_+\Gamma_-)^6 = 1$ the monodromy

group is isomorphic to Z_6. This means, that $f_+(z)$ and $f_-(z)$ are single-valued functions of the variable

$$t = \left(\frac{zb^{-1} - 1}{1 - zb^{-1*}}\right)^{1/6}. \tag{11}$$

These functions may have singularities at the points, corresponding to $z = 0, \infty$ and at $t = 0, \infty$. This information, together with the monodromy transformation rules (10) is sufficient to solve the (9) (see appendix C). The functions $f_+(z)$ and $f_-(z)$ correspond to different sheets of the Riemann surface of the same function $f_\pm$:

$$f_\pm = \left(\frac{t + t^{-1}}{\sqrt{3}} + C(t + t^{-5}) + C^*(t^{-1} + t^5)\right) z^{-1} \tag{12}$$

where C is an unknown complex constant, and the phase of the variable t is chosen at $z = 0$ equal to $+\pi/6$ for f_+ and $-\pi/6$ for f_-. Recall now that the monodromy properties (10) hold only when the curves Ψ and Ξ do not intersect. These curves are defined by the condition that the forms $f_-\mathrm{d}z$ and $f_+\mathrm{d}z$ have purely imaginary values on the vectors, tangent to Ψ and Ξ, respectively (see equation (6)). The simple analysis shows, that the non-intersection condition is satisfied only at $C = 0$. Thus, for $b_+ = b_-$ we have

$$f_\pm(z) = \left(\frac{t + t^{-1}}{\sqrt{3}}\right) z^{-1}. \tag{13}$$

Although the parameter C is redundant in the case $b_+ = b_-$, it describes, as shown below, the perturbations of $f_\pm$ under small changes of n_+, n_- and Δ.

Consider first the case of symmetry between left and right particles. This symmetry imposes the conditions $n_- = n_+$, $b = \mathrm{i}|b|$ and ϕ, $\Delta = 0$. Denote the densities of left and right particles n_+/M and n_-/M in the thermodynamic limit by Q_- and Q_+:

$$Q_\pm = \lim_{M\to\infty} \frac{n_\mp}{M}. \tag{14}$$

These densities are defined by the residues of $f_+(z)\,\mathrm{d}z$ and $f_-(z)\,\mathrm{d}z$ at $z = \infty$:

$$\mathrm{res}\,(f_\pm \mathrm{d}z)|_{z=\infty} = Q_\pm - 1 \tag{15}$$

and are both equal in this case to $1 - 1/\sqrt{3}$. These densities, together with the condition $\Delta = 0$ correspond to zero phason gradient (see appendix B). A simple algebra then gives entropy per one vertex for this case (see appendix C):

$$\sigma_{v0} = \log(108) - 2\sqrt{3}\,\log(2 + \sqrt{3}) = 0.120\,055\,249\,318\,541\ldots \tag{16}$$

which is close to the value 0.120 055 249 315(6) found numerically by Widom [8]. However, the assertion [8] that in the thermodynamic limit of the 12-fold-symmetric phase $p_1, p_{n_+}, q_1, q_{n_-} \to \pm\pi/4$ is erroneous. Indeed, this should mean that $b = \mathrm{i}$, but this is not the case: $b = \mathrm{i}6\sqrt{3}(2 - \sqrt{3})^{\sqrt{3}} = 1.060\ldots\mathrm{i}$.

Apply now a small phason gradient having 4-fold symmetry, imposing $Q_+ = Q_- = 1 - 1/\sqrt{3} - \epsilon$, $\Delta = 0$. Then a gap appears between b_+ and b_-. Nevertheless, we can still use the variable t, defined in (11), where now $b = (b_+ + b_-)/2$. In this case f_- and f_+ are single-valued functions of t except two small regions $|t| \sim |b_+ - b_-|^{1/6}$ and $|t|^{-1} \sim |b_+ - b_-|^{1/6}$ around the points $t = 0$ and $t = \infty$. This gives rise to the singularities in the first-order correction to $f_\pm$ in ϵ at the points $t = 0, \infty$. As t approaches 'bad' regions around 0 and ∞, this correction turns comparable with $f_\pm$. The maximum entropy condition means, as can easily be shown, that we have to maximize ϵ for a given $|b_+ - b_-|$, or, reciprocally, to minimize $|b_+ - b_-|$ keeping ϵ constant. Thus, among all corrections

to $f_\pm$ satisfying the condition $Q_+ = Q_- = 1 - 1/\sqrt{3} - \epsilon$ we should select that having the weakest singularities at $t = 0, \infty$. On the other hand, we have seen, that the condition of slow growth of $f_\pm$ at $t = 0, \infty$ leaves the complex parameter C in (12) indeterminate. Evidently, the terms in (12) proportional to C and C^* give the least singular correction to $f_\pm$. The condition $Q_+ = Q_- = 1 - 1/\sqrt{3} - \epsilon$ is satisfied when $C = \epsilon/2$, which gives (see appendix C)

$$\sigma_v = \sigma_{v0} - 3\sqrt{3}\log(2+\sqrt{3})\epsilon^2 + o(\epsilon^2). \tag{17}$$

One can remark that the terms of the first order in ϵ do not appear in (17) and that the coefficient at ϵ^2 is negative, conforming to the assumption that the entropy reaches its maximum on tilings with 12-fold symmetry. Taking into account that the entropy per unit area σ_a is expressed in terms of σ_v as

$$\sigma_a = \left(1 + (2/\sqrt{3} - 1)\alpha_t\right)\sigma_v \tag{18}$$

we obtain one of the phason-elasticity constants K_ξ (see [8, 9]):

$$K_\xi = (2-\sqrt{3})\left(\log(108)/\sqrt{3} + 2\log(2+\sqrt{3})\right) = 1.430\,083\,831\,75\ldots \tag{19}$$

which is close to the estimation $K_\xi = 1.430\,083\,830\,79(3)$ found in [8].

It is worth mentioning here that this result cannot be obtained by the formal decomposition of the correction to $f_\pm$ in powers of $b_+ - b_-$. Indeed, the fact that the correction turns comparable with $f_\pm$ when $|t| \sim |b_+ - b_-|^{1/6}$ or $|t^{-1}| \sim |b_+ - b_-|^{1/6}$ corresponds to the scaling

$$|\epsilon| \sim |b_+ - b_-|^{2/3} \tag{20}$$

i.e. the correction to $f_\pm$ is singular with respect to $b_+ - b_-$.

Consider now the case $b_+ = b_- = \mathrm{i}|b|\mathrm{e}^{-\mathrm{i}\gamma}$. Calculations of the residues of $f_\pm$ from (12) at $z = \infty$ give

$$Q_\pm = 1 - \frac{2}{\sqrt{3}}\cos\frac{\pi \pm \gamma}{3} \tag{21}$$

which is consistent with the 6-fold symmetry of the phason gradient (see appendix B). It remains to calculate Δ, which must be equal to 0 for the case of the 6-fold symmetry. As a thermodynamic conjugate to the variable ϕ, Δ is equal to the first derivative of the free energy per row with respect to ϕ. The calculation of this derivative can be performed in the same way as the calculation of the first-order correction in ϵ in (17) and gives 0 (see appendix C). Thus, one obtains the expression for σ_v for *all* phason gradients having 6-fold symmetry:

$$\sigma_v = \log\left(\frac{108}{\cos^2\gamma}\right) + \sqrt{3}\cos\left(\frac{\gamma}{3}\right)\log\left(\frac{2\cos(\gamma/3) - \sqrt{3}}{2\cos(\gamma/3) + \sqrt{3}}\right) - \sin\left(\frac{\gamma}{3}\right)\log\left(\frac{2 - \cos(2\gamma/3) + 3\sin(\gamma/3)}{2 - \cos(2\gamma/3) - 3\sin(\gamma/3)}\right) \tag{22}$$

where γ is related with n_- and n_+ by (21). It is convenient to express γ in terms of the area fraction α_t:

$$\sin\frac{\gamma}{3} = \frac{\sqrt{2\alpha_t - 1}}{\sqrt{3} + (2-\sqrt{3})\alpha_t}. \tag{23}$$

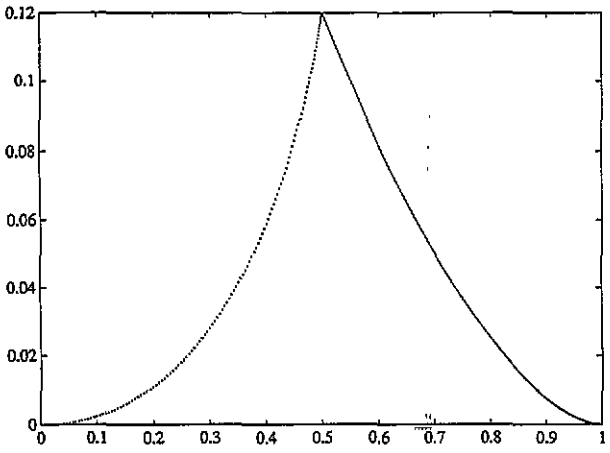

Figure 5. The entropy per one vertex as a function of α_t. The left part of the plot is the numerical result for $M = 627$ and the right part is analytic (see (22) and (23)).

Decomposing (22) and (23) at $\gamma = 0$ one can obtain the second phason elasticity constant [8, 9] (see appendix B):

$$K_\mu = 2\sqrt{3} - 3 = 0.464\,101\,615\ldots, \tag{24}$$

This value differs by 1% from that found in [8]. The author supposes that this difference stems from the fact that in [8] maximization of the entropy per unit area is erroneously identified with the maximization of the largest eigenvalue of the transfer matrix. As discussed above, this is true only when the area scaling factor in the lattice representation of the model depends only on α_t, and this is not the case for the representation, used in [8].

Recalling that at $\alpha_t > \frac{1}{2}$ the entropy reaches its maximum on the tilings with 6-fold symmetry, we conclude that (22) and (23) give the function $\sigma_v(\alpha_t)$ for $\alpha_t > \frac{1}{2}$. This function is plotted in figure 5 together with the results of numerical calculations for the case of 4-fold symmetry ($\alpha_t < \frac{1}{2}$).

4. Discussion

The square-triangle random-tiling model appears to be solvable analytically in the thermodynamic limit for the phason strains having 6-fold symmetry. In what follows, the results of this solution and the open questions are discussed.

One can remark that the curve $\sigma_v(\alpha_t)$ (see figure 5) is concave on the segments $0 < \alpha_t < \frac{1}{2}$ and $\frac{1}{2} < \alpha_t < 1$. Moreover, the curve $\sigma_a(\alpha_t)$, which is not shown here, possesses the same property. This should mean that all phases of the square-triangle random-tiling model except the perfect triangular and square lattices and the phase having 12-fold symmetry are absolutely unstable! This seems to be doubtful, because the Monte Carlo simulations show the stability of the phases with any value of α_t [4]. In fact this apparent contradiction is due to an unphysical feature of the model, forbidding the system from phase separation. Indeed, the phases having different values of phason gradient are always separated by an 'intermediate phase', which is present in amounts, comparable to the amount of those firsts. In any real system these constraints are cancelled by the presence of defects, no matter how high the energy cost of the defects is.

The solutions of the Bethe-ansatz equations (4) differ qualitatively in the case of 6-fold-symmetric background phason strain and in other cases. In the 6-fold symmetric case the distribution of the momenta p_i and q_j is singular near their limiting values: as follows from

(13), the density of states diverges as $|p-p_{\text{edge}}|^{-1/6}$ (see figure 3). Thus, the question arises as to whether the 6-fold-symmetric tilings are really set off all others, or is this singularity just an artefact due to improper choice of the coordinate system. Because the dependence of the entropy density on the phason strain is regular in the vicinity of the line of 6-fold symmetry at least up to the terms of second order, one could suppose the latter. The author, however, interprets this phenomenon as an indication of the presence of 'hidden' macroscopic parameters (or *slow variables*), in addition to the phason field. Although the very notion of the slow variable is not rigorously defined, it is generally supposed that a complete set of these variables fixes the microscopic state of a system up to purely local degrees of freedom. The phason field for the square-triangle tiling, however, does not satisfy this condition. Indeed, switching of a 'zipper' (see the definition of this object in [4]) cannot be decomposed into a sequence of *local* rearrangement of tiles, without creation of defects. On the other hand, two tilings, differentiated by the state of a 'zipper', are macroscopically identical. To illustrate the aforementioned, one can compare the square-triangle tiling and the dimer model on the honeycomb lattice. The latter has much in common with the random-tiling QC models; in particular, it allows the description by an analogue of the phason field [10]. This field satisfies the condition on the complete set of slow variables, formulated above. The analogy with the square-triangle tiling model can be pursued because the dimer model on the honeycomb lattice, mapped by Wu [11] onto the 6-vertex model, can be solved by the Bethe-ansatz technique, too [12]. This solution, however, reveals no singularity in the distribution of the momenta of particles for any value of the background 'phason' strain.

Acknowledgments

The author is grateful to M Widom, C Henley and A Neveu for useful discussions. He also wishes to thank Groupe de dynamique des phases condensées at Université Montpellier 2 and Laboratoire de Thermodynamique et Physico-Chimie Métallurgique at CNRS for their hospitality and support.

Appendix A

Equation (2) for the amplitudes of the partial waves $A(\{k_i\})$ defines unambiguously the ratio $A(\{\mathcal{P}(k_i)\})/A(\{k_i\})$ for an arbitrary permutation $\mathcal{P}$. These equations are suited to the requirements of one- and two-particle processes, and their compatibility with multi-particle scattering is a non-trivial issue. The proof of the validity of (2) for multi-particle processes is given in what follows.

The equation on the eigenstate of the transfer matrix is

$$\Lambda \mathcal{A}_{\{z_j'\}} = \sum_{\{z_i\}} T_{\{z_j'\}\{z_i\}} \mathcal{A}_{\{z_i\}} \tag{A.1}$$

where Λ is given by (1) and the amplitudes in the coordinate space are

$$\mathcal{A}_{\{z_i\}} = \sum_{\{k_i\}} A(\{k_i\}) \exp\left(\mathrm{i} \sum_n k_n z_n\right). \tag{A.2}$$

Consider first the special case of the configuration $\{z_j'\}$, in which all particles are separated by distances over 2. As there is no interaction between particles, the sum in the RHS of (A.1) comprises only one non-zero term. Because Λ in (1) is a product of single-particle contributions, (A.1) holds for $\{z_j'\}$ of the sort.

For an arbitrary configuration $\{z'_j\}$ the number of non-zero terms in the RHS of (A.1) is equal to 2^L, where L is the number of *elementary clusters*, like that shown in figure A1(a). Any of these clusters can originate from two configurations, as shown in figures A1(b) and (c). Because the contributions of elementary clusters in (A.1) are multiplicative, it will suffice to consider only one of them. Let it comprise k_+ left and k_- right particles having coordinates $\{-2k_+ + 1, \ldots, -1\}$ and $\{1, \ldots, 2k_- - 1\}$, respectively. Equation (A.1) becomes

$$A_0 \prod_{i,j}(\xi_i - \psi_j) = A_0\left(\sum_\alpha (-1)^{k_+-\alpha} \xi_\alpha^{k_-} \prod_{\substack{i,j \\ i\neq\alpha}} (\xi_i - \psi_j) \prod_{n\neq\alpha} \xi_n^{-1}\right)$$
$$+ A_0\left(\sum_\beta (-1)^{k_+ + k_- - \beta} \psi_\beta^{k_+} \prod_{\substack{i,j \\ j\neq\beta}} (\xi_i - \psi_j) \prod_{n\neq\beta} \psi_n^{-1}\right) \tag{A.3}$$

where

$$A_0 = A(q_1, \ldots, q_{k_-}, p_{k_+}, \ldots, p_1) \prod_{m<n} (\xi_m^{-1} - \xi_n^{-1}) \prod_{m<n} (\psi_m^{-1} - \psi_n^{-1})$$
$$\times \exp\left(\frac{k_+(k_+ - 1) - k_-(k_- - 1)}{2}\phi\right)$$

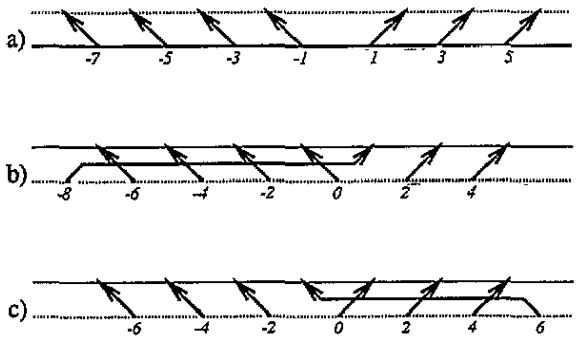

Figure A1. (a) The *elementary cluster* ($k_+ = 4$ and $k_- = 3$), and two configurations of particles, which can precede it (b) and (c).

and ψ_j, ξ_i are given by (3). Multiplying (A.3) by

$$A_0^{-1} \prod_{n_1} \xi_{n_1}^{k_+-1} \prod_{n_2} \psi_{n_2}^{k_- - 1}$$

gives

$$W(\psi_1, \ldots, \psi_{k_-}, \xi_1, \ldots, \xi_{k_+})$$
$$= \sum_\beta W(\psi_1, \ldots, \hat{\psi}_\beta, \ldots, \psi_{k_-}, \xi_1, \ldots, \xi_{k_+}) \psi_\beta^{k_+ + k_- - 1} (-1)^{k_+ + k_- - \beta}$$
$$+ \sum_\alpha W(\psi_1, \ldots, \psi_{k_-}, \xi_1, \ldots, \hat{\xi}_\alpha, \ldots, \xi_{k_+}) \xi_\alpha^{k_+ + k_- - 1} (-1)^{k_+ - \alpha} \tag{A.4}$$

where W is a Vandermonde determinant,

$$W(x_1, \ldots, x_n) = \det \begin{pmatrix} 1 & . & . & . & x_1^{n-1} \\ . & . & . & . & . \\ . & . & . & . & . \\ . & . & . & . & . \\ 1 & . & . & . & x_n^{n-1} \end{pmatrix}$$

and the hat over a symbol denotes its omission. As (A.4) is nothing but a Laplace expansion of $W(\psi_1, \ldots, \xi_{k_+})$ in the minors of the first order, the identity (A.1) is obeyed for any configuration $\{z_j'\}$. Thus, the Bethe ansatz (A.2) with amplitudes $A(\{k_i\})$ satisfying (2) gives the exact eigenstates of the transfer matrix.

Appendix B

This appendix is concerned with purely geometrical relations between different parameters, describing the background phason strain. The consideration is restricted to the special cases of the 6-fold and 4-fold symmetries.

As the background phason strain parameters and the area fraction α_t are insensitive to local rearrangements of tiles, it will suffice to consider only one representative for any phason strain. It is convenient to choose the periodic tilings, shown in figure B1. Although these tilings exist only while x and y are integers, one can formally continue the results to arbitrary real values of x and y.

Consider first the case of the 6-fold symmetry (figure B1(a)). The densities of right and left particles are equal to

$$Q_+ = \frac{3x^2 + x}{3x^2 + 3x + 1} \qquad Q_- = \frac{x + 1}{3x^2 + 3x + 1}. \tag{B.1}$$

The area fraction α_t is given by

$$\alpha_t = \frac{3x^2 + 1}{(\sqrt{3}x + 1)^2}. \tag{B.2}$$

Because the substitution

$$x = \frac{\sin\gamma/3 + (\cos\gamma/3)/\sqrt{3}}{1 - 2\sin\gamma/3} \tag{B.3}$$

transforms (B.1) into (21), the densities of particles, given by (21), are compatible with the 6-fold symmetry of the phason strain. The relation (23) between the parameters α_t and γ follows from (B.2) and (B.3).

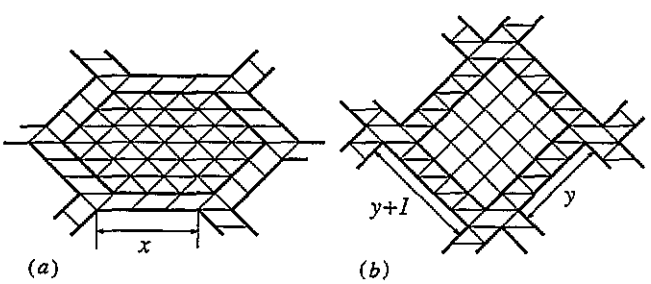

Figure B1. Periodic tilings, having (a) 6-fold and (b) 4-fold symmetries ($x = 3$ and $y = 4$). Both tilings are shown in the lattice representation (see figure 2).

The 4-fold symmetry requires $n_+ = n_-$, while the reflection symmetry gives also $\Delta = 0$. An example of periodic tiling, having this symmetry is shown in figure B1(b). The densities of right and left particles are given by

$$Q_+ = Q_- = \frac{1}{y + 2} \tag{B.4}$$

while the area fraction equals

$$\alpha_t = \frac{\sqrt{3}(2y + 1)}{2y^2 + (2 + 2\sqrt{3})y + 2 + \sqrt{3}}. \tag{B.5}$$

Zero background phason strain corresponds to $x = \sqrt{3}/3$ and $y = (\sqrt{3}-1)/2$. Thus, the densities of particles in this case are

$$Q_+ = Q_- = 1 - \frac{\sqrt{3}}{3}$$

and the area fraction α_t equals $\frac{1}{2}$.

Consider now the quadratic invariants in phason strain [4, 8]. The action of the 12-fold-symmetry group on the space of the phason gradients (see figure 1) leaves invariant two subspaces. One of them, two-dimensional, corresponds to 4-fold-symmetric phason strains, the other, one-dimensional, to 6-fold-symmetric strains. Hence, there are two independent quadratic invariants in phason gradients. It would be reasonable to choose as these invariants the squares of the 4-fold and the 6-fold-symmetric components of the phason strain. Unfortunately, of the invariants I_ξ and I_μ already introduced in [4, 8, 9] only I_μ meets this condition. In fact, as follows from formula (9) of [8], I_μ vanishes on 4-fold-symmetric phason strains. The second 'natural' invariant should vanish on the 6-fold-symmetric subspace. As is clear from equations (9) and (10) of [8], the linear combination:

$$\tilde{I}_\xi = I_\xi + \tfrac{1}{4} I_\mu \tag{B.6}$$

possesses the desired property. Express the invariants I_μ and $\tilde{I}_\xi$ in terms of other parameters, describing the phason strain. In doing so, one can use the relation

$$\alpha_t = \tfrac{1}{2} - \tfrac{1}{2} I_\xi \tag{B.7}$$

which is valid at least up to the second order in phason strain (Henley [13] argues that the definition of I_ξ given in [4] makes (B.7) exact).

Consider first 6-fold-symmetric phason strains, which are described by the parameter γ. As follows from (23) and (B.7),

$$I_\xi = -\gamma^2 \frac{(2+\sqrt{3})^2}{36}.$$

On the other hand, as the 'natural' parameter $\tilde{I}_\xi$ equals 0 in the case being considered, I_μ is given by

$$I_\mu = \gamma^2 \frac{(2+\sqrt{3})^2}{9}. \tag{B.8}$$

The invariant $\tilde{I}_\xi$ characterizes the 4-fold-symmetric component in phason strain. It is convenient to express it in terms of ϵ, the deviation of the density of the right and left particles from $1 - \sqrt{3}/3$:

$$\epsilon = 1 - \frac{\sqrt{3}}{3} - Q_\pm. \tag{B.9}$$

The formulae (B.4), (B.5) and (B.9) allow one to express α_t in terms of ϵ. Decomposing of α_t up to the second order in ϵ yields

$$\alpha_t = \frac{1}{2} - \frac{3(2+\sqrt{3})^2}{8}\epsilon^2.$$

Taking into account (B.6) and (B.7), one obtains

$$\tilde{I}_\xi = \frac{3(2+\sqrt{3})^2}{4}\epsilon^2 \tag{B.10}$$

(recall, that $I_\mu = 0$ for 4-fold-symmetric phason strains).

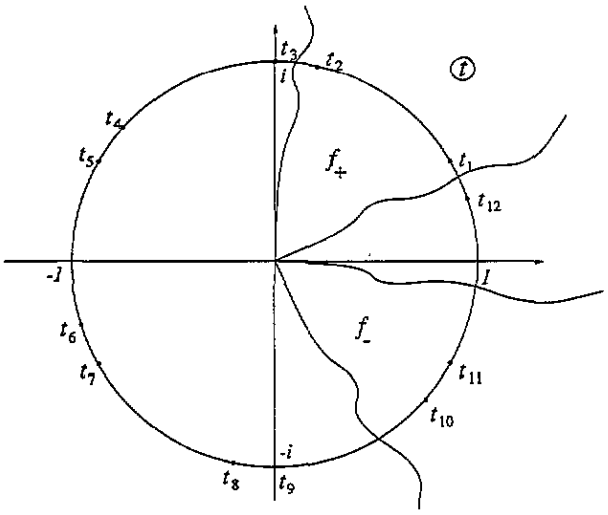

Figure C1. The poles of the form $f_{\pm}dz$ and the sectors, corresponding to f_+ and f_- in the plane of the variable t.

Appendix C

This appendix describes, in brief, how the use of the monodromy properties of f_+ and f_- can help one to solve (9). In what follows it is also shown how the entropy density (22) and the phason elastic constants (19) and (24) were calculated.

The functions f_+ and f_- can be continued analytically beyond their cuts by the monodromy transformations (10). Because the monodromy element $\Gamma_+\Gamma_-$ transforms f_- into f_+, they correspond to different branches of the same analytic function, denoted by $f_{\pm}$. As discussed above, when $b_+ = b_- = i|b|e^{-i\gamma}$, the Riemann surface of $f_{\pm}$ consists of six sheets, which can be mapped into a plane by the substitution (11). Consider the analytical properties of $f_{\pm}dz$ as a 1-form in the plane of the variable t. The finiteness of the number of particles implies the absence of the singularities in $f_{\pm}dz$ at $t = 0, \infty$. Hence, there are no singularities other than the simple poles at the points, corresponding to $z = 0, \infty$, i.e. the form $f_{\pm}dz$ is rational in the variable t. These points are listed in table 1, along with the residues of $f_{\pm}dz$ at these points. The poles t_1 and t_2 belong to the sheet of the Riemann surface of $f_{\pm}$, corresponding to f_+, while t_{10} and t_{11} belong to the sheet, corresponding to f_- (see figure C1). As $z(t_1) = z(t_{11}) = 0$ (see equation (11)), the residues at them are both equal to 1. The residues r_2 and r_{10} are given by (15). All other residues in table 1 are calculated from these four by application of the monodromy transformation rules (10). These numbers define $f_{\pm}dz$ unambiguously:

$$f_{\pm}dz = \sum_{n=1}^{12} r_n \frac{dt}{t - t_n}.$$

This expression is equivalent to (12) if

$$Q_{\pm} = 1 - \frac{2}{\sqrt{3}}\cos\frac{\pi \pm \gamma}{3} - 2\mathrm{Re}\,C\left(\cos\frac{\pi \pm \gamma}{3} + \cos\frac{5(\pi \pm \gamma)}{3}\right) + 2\mathrm{Im}\,C\left(\sin\frac{\gamma \pm \pi}{3} - \sin\frac{5(\gamma \pm \pi)}{3}\right). \tag{C.1}$$

Consider now the calculation of the entropy density (22) (formula (16) is the special case of (22) when γ equals 0). The entropy per one vertex σ_v and the maximal eigenvalue

Table C1. The poles and residues of the form $f_{\pm}\mathrm{d}z$.

Pole	t	z	r_π, residue of $f_{\pm}(z)\,\mathrm{d}z$
t_1	$e^{\pi i/6}$	0	1
t_2	$e^{(\pi+\gamma)i/3}$	∞	$Q_+ - 1$
t_3	i	0	0
t_4	$e^{(2\pi+\gamma)i/3}$	∞	$1 - Q_-$
t_5	$e^{5\pi i/6}$	0	-1
t_6	$-e^{i\gamma/3}$	∞	$2 - Q_+ - Q_-$
t_7	$-e^{\pi i/6}$	0	-1
t_8	$-e^{(\pi+\gamma)i/3}$	∞	$1 - Q_+$
t_9	$-i$	0	0
t_{10}	$e^{(\gamma-\pi)i/3}$	∞	$Q_- - 1$
t_{11}	$e^{-\pi i/6}$	0	1
t_{12}	$e^{i\gamma/3}$	∞	$Q_+ + Q_- - 2$

Λ of the transfer matrix are related by

$$\sigma_{\mathrm{v}} = \lim_{M\to\infty} M^{-1}(\log\Lambda - \phi\Delta) \tag{C.2}$$

where Δ, the average difference between the numbers of 'right' and 'left' intersections of the world lines of the particles in a row, is given by

$$\Delta = \frac{\partial \log\Lambda}{\partial\phi}.$$

Λ can be expressed in terms of $\{\xi_l\}$ and $\{\psi_j\}$ in the following way:

$$\lim_{M\to\infty} M^{-1}\log\Lambda = \frac{s_+ + s_-}{2} + \frac{Q_+ - Q_-}{2}\phi \tag{C.3}$$

where

$$s_+ = \lim_{M\to\infty} M^{-1}\sum_j \log|\psi_j| \qquad s_- = \lim_{M\to\infty} M^{-1}\sum_l \log|\xi_l|. \tag{C.4}$$

For brevity, it is convenient to introduce the following forms:

$$g_+\mathrm{d}z = \left(\frac{r_2}{t-t_2} + \frac{r_8}{t-t_8}\right)\mathrm{d}t \qquad g_-\mathrm{d}z = \left(\frac{r_4}{t-t_4} + \frac{r_{10}}{t-t_{10}}\right)\mathrm{d}t$$
$$h_+\mathrm{d}z = \left(\frac{r_1}{t-t_1} + \frac{r_7}{t-t_7}\right)\mathrm{d}t \qquad h_-\mathrm{d}z = \left(\frac{r_5}{t-t_5} + \frac{r_{11}}{t-t_{11}}\right)\mathrm{d}t.$$

Equation (6) and its analogue for $\{\psi_j\}$ allow one to write

$$\begin{aligned} J_{+,\infty} &= \mathrm{Re}\int_b^{\infty}(f_+ - g_+)\,\mathrm{d}z = (Q_+ - 1)\log\frac{6}{|b|} - \phi \\ J_{-,\infty} &= \mathrm{Re}\int_b^{\infty}(f_- - g_-)\,\mathrm{d}z = (Q_- - 1)\log\frac{6}{|b|} + \phi. \end{aligned} \tag{C.5}$$

On the other hand, equations (C.4) give

$$\begin{aligned} J_{+,0} &= \mathrm{Re}\int_b^{0}(f_+ - h_+)\,\mathrm{d}z = \log 6|b| - s_+ \\ J_{-,0} &= \mathrm{Re}\int_b^{0}(f_- - h_-)\,\mathrm{d}z = \log 6|b| - s_-. \end{aligned} \tag{C.6}$$

The integrals in (C.5) and (C.6) can easily be taken in the plane of the variable t:

$$J_{+,\infty} = \sum_{n\neq 2,8} r_n \log|t_n - t_2| \qquad J_{-,\infty} = \sum_{n\neq 4,10} r_n \log|t_n - t_{10}|$$

$$J_{+,0} = \sum_{n\neq 1,7} r_n \log|t_n - t_1| \qquad J_{-,0} = \sum_{n\neq 5,11} r_n \log|t_n - t_{11}|$$

(recall that all r_n are real numbers). Equations (C.3), (C.5) and (C.6) give

$$\lim_{M\to\infty} M^{-1} \log \Lambda = \log 36 - \frac{J_{+,0} + J_{-,0}}{2} - \frac{J_{+,\infty} + J_{-,\infty}}{Q_+ + Q_- - 2} + \frac{J_{+,\infty}(Q_+ - 1) + J_{-,\infty}(Q_- - 1)}{2}. \tag{C.7}$$

The densities of the particles Q_+ and Q_- are given by (C.1). The differentiation of (C.7) with respect to C at $C = 0$ gives 0. As noted above, this corresponds to

$$\frac{\partial}{\partial \phi} \log \Lambda|_{C=0} = 0. \tag{C.8}$$

Finally, equations (C.2), (C.7) and (C.8) give the formula for the entropy per one vertex (22).

Consider now the calculation of the phason elasticity constants K_ξ and K_μ. In [8] it is claimed that they both are the two principal curvatures of the entropy density with respect to characteristic symmetry-breaking phason strains, but this is the case only for the constant K_ξ. In fact, the decomposition of the entropy per unit area near its maximum, given by the formula (6) of [8] can be rewritten in terms of the 'natural' invariants as

$$\sigma_a = \sigma_{a0} - \tfrac{1}{2} K_\xi \tilde{I}_\xi - \tfrac{1}{2}\left(K_\mu - \tfrac{1}{4} K_\xi\right) I_\mu \ldots \tag{C.9}$$

where the ellipsis denotes terms of third and higher orders in phason strain.

As is clear from (C.9), the constant K_ξ specifies the phason elasticity with respect to 4-fold-symmetric phason strains. These strains are in the first order described by the parameter ϵ in (B.9). Thus, the arithmetics of the constant K_ξ requires a consideration of the first- and second-order corrections to $f_\pm$ in ϵ. The first-order terms are given by (12), where $C = \epsilon/2$. As for the terms of the second order in ϵ, there is good reason to believe that they are equal to 0. This point, being a vital issue in the calculations, merits detailed consideration.

The calculation of K_ξ would present no problems if the equations (9) were solved exactly in the general case, when $b_+ \neq b_-$. Although they were not, the monodromy transformations (10) may tell the following about the structure of the solution: (i) the Riemann surface of the function $f_\pm$ consists of infinite number of sheets, which can be labelled by the elements of $SL(2, Z)$; (ii) the form $f_\pm dz$ has two poles on each sheet at the points $z = 0$ and $z = \infty$, whose residues can be calculated exactly; (iii) while $b_+ = b_-$ the Riemann surface of $f_\pm$ is degenerate, namely it is decomposed into disconnected parts, comprising six sheets each. Small 4-fold-symmetric phason strain, specified by the parameter ϵ (B.9) affects both the values of the residues of $f_\pm dz$ and the topology of the Riemann surface of $f_\pm$. Because the monodromy elements Γ_+ and Γ_- can act separately when $b_+ \neq b_-$, the parts of Riemann surface, so far disconnected, become joined by narrow necks of width $|b_+ - b_-| \sim \epsilon^{3/2}$ (20). As for the residues, the corrections to all them are linear in ϵ. The formula (12) ignores the modification to the topology, but it should be taken into account in the calculations in the next order in ϵ. Since it is the entropy density which is of most interest, one should consider the corrections to the integrals (C.5) and (C.6) caused by the changes in the topology of the Riemann surface of $f_\pm$. These corrections arise from the contribution of the poles, lying

on other parts of the Riemann surface. Because the net residue of $f_{\pm}dz$ on each part of the surface equals zero, this contribution away from the points $z = b_-, b_+$ is proportional to $|b_+ - b_-|^2 \sim \epsilon^3$. In other words, there is no correction of second order in ϵ to the integrals (C.5) and (C.6).

All the above implies that the decomposition of the expression (C.7) up to the terms of the second order in $\mathrm{Re}\,C$ at $C = 0$

$$\lim_{M\to\infty} M^{-1}\log\Lambda = \log 108 - 2\sqrt{3}\log(2+\sqrt{3}) - 12\sqrt{3}\log(2+\sqrt{3})(\mathrm{Re}\,C)^2 + o(\mathrm{Re}\,C)^2 \tag{C.10}$$

suffice to calculate the elastic constant K_ξ. The formula (17) follows from (C.2), (C.10) and from the fact that the 4-fold symmetry with reflection requires $\phi = 0$. Because $\tilde{I}_\xi$ is related to ϵ by (B.10), the correction to the entropy per one vertex is

$$\sigma_v = \sigma_{v0} - \tfrac{1}{2}\tilde{I}_\xi\left((56\sqrt{3} - 96)\log(2+\sqrt{3})\right).$$

As the factor between the entropy per unit area and σ_v depends on α_t (see the formula (18)), it's derivative with respect to α_t also contributes to K_ξ:

$$K_\xi = -2\left(\frac{\partial\sigma_v}{\partial\tilde{I}_\xi}\bigg|_{\tilde{I}_t=+0} + \left(\frac{2}{\sqrt{3}} - 1\right)\sigma_{v0}\frac{\partial\alpha_t}{\partial\tilde{I}_\xi}\bigg|_{\tilde{I}_t=+0}\right). \tag{C.11}$$

The expression (19) follows from (C.11) and (B.7).

Decomposing (22) up to the second order in γ and taking into account the relation between I_μ and γ (B.8) we obtain the second 'natural' phason elasticity coefficient:

$$K_\mu - \tfrac{1}{4}K_\xi = \frac{\sqrt{3}(2-\sqrt{3})}{12}\left(12 - \log(108) - 2\sqrt{3}\log(2+\sqrt{3})\right) \tag{C.12}$$

(as in the case of K_ξ, the terms coming from the scaling factor (18) should be taken into account). The result (C.12) combined with the expression for K_ξ (19) gives (24).

References

[1] Kasteleyn P V 1961 *Physica* **27** 1209
[2] Baxter R J 1982 *Exactly Solved Models in Statistical Mechanics* (New York: Academic)
[3] Elser V 1985 *Phys. Rev.* B **32** 4892
[4] Oxborrow M and Henley C L 1993 *Phys. Rev.* B **48** 6966
[5] Henley C L 1990 *Quasicrystals and Incommensurate Structures* ed M J Yakaman *et al* (Singapore: World Scientific) p 152
[6] Lei Han Tang 1989 *Mod. Phys. Lett.* B **3** 1121
[7] Socolar J E S and Steinhardt P J 1986 *Phys. Rev.* B **34** 3345
[8] Widom M 1993 *Phys. Rev. Lett.* **70** 2094
[9] Henley C L and Oxborrow M 1993 *J. Non-cryst. Solids* **153–154** 210
[10] Elser V 1984 *J. Phys. A: Math. Gen.* **17** 1509
[11] Wu F Y 1968 *Phys. Rev.* **168** 539
[12] Lieb E H 1967 *Phys. Rev.* **162** 162
[13] Henley C L 1993 private communication